This is the author's version of an article that has been published in this journal. Changes were made to this version by the publisher prior to publication.
The final version of record is available at http://dx.doi.org/10.1109/JSEN.2021.3062428

Comments on "SPICE Model of Photomultiplier Tube Under Different Bias Conditions"

Fernando Hueso-González, Damián Ginestar, José L. Hueso, and Jaime Riera

***Abstract*— The paper "SPICE Model of Photomultiplier Tube Under Different Bias Conditions" is commented. We revisit the mathematical formulation to compensate for some ambiguities in the original manuscript, and point out some inconsistencies in the results and reproducibility of the simulations, as well as in the optimized parameters originally obtained with the PSPICE simulation engine. All simulations are recalculated with the NGSPICE software using the corrected parameters and compared against the original figures. The reproducibility of our simulations is independently verified with PSPICE, as well as by numerically solving the analytical system of non-linear equations using Newton's method within MATLAB.**

***Index Terms*— MODL, OPTO**

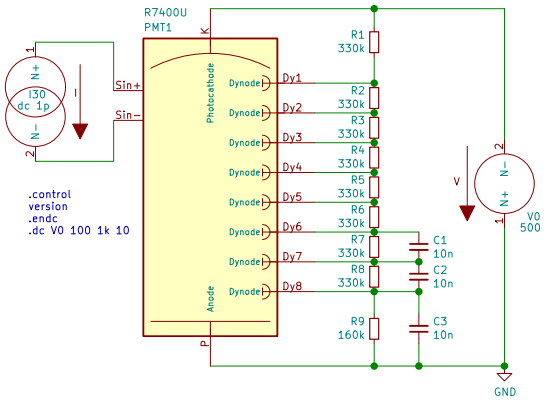

I. Introduction

THE behavioral modeling of a Photomultiplier Tube (PMT) using Simulation Program with Integrated Circuit Emphasis (SPICE) was proposed in [1] and applied later in [2]. The author predicted the non-linearity of the PMT gain [3], [4] for different photocathode currents and divider networks, as well as the inter-dynode voltages under static illumination conditions, and compared the simulation results to experimental measurements [5].

The SPICE model proposed by [1] is a very useful tool for studying the theoretical response of PMTs to arbitrary illumination conditions and for different voltage bias networks [5]. This relevant study has a broad number of applications. For example, it is essential in the field of prompt gamma-ray measurements during proton therapy with scintillation detectors coupled to PMTs [6], [7], where large count rate variations affect the stability of the gain [8].

In this comment, we address some ambiguities in the mathematical description of the aforementioned SPICE model and point out at some inconsistencies between the optimized parameters deployed in the simulation and the analytical predictions. We recalculate all results using two independent SPICE simulation engines: the open-source NGSPICE simulator [9] (version 33+) and the commercial OrCAD PSPICE software [10] by Cadence (version 17.4). We then verify the reproducibility of the results published in the original manuscript. For completeness, we also enunciate the analytical equations that describe the node voltages in the circuit and solve numerically the resulting system of nonlinear equations with MATLAB [11] by MathWorks (version 2019b).

Manuscript submitted on January 29, 2021. This work was supported by Conselleria de Educación, Investigación, Cultura y Deporte (Generalitat Valenciana) under grant number CDEIGENT/2019/011.

F Hueso-González is with Instituto de Física Corpuscular (CSIC / UVEG), c/ Catedrático José Beltrán 2, 46980 Paterna, Spain (e-mail: fernando.hueso@uv.es).

D Ginestar, JL Hueso, and J Riera are with Instituto de Matemática Multidisciplinar. Universitat Politècnica de València. Camí de Vera, s/n. 46022 València. Spain. (e-mail: dginesta@mat.upv.es, jlhueso@mat.upv.es, jriera@fis.upv.es).

II. Theoretical Background

A PMT [12] is a non-thermionic vacuum tube consisting of $N+2$ electrodes, namely one cathode, N dynodes and one anode (see Fig. 1). An ideal cathode ($i = 0$) emits electrons proportionally to the incident light thanks to the photoelectric effect. The dynodes ($i = 1, \ldots, N$) act as successive amplification stages of the emitted photoelectrons via secondary emission [13]. The anode ($i = N+1$) does not amplify further, but rather collects the current emitted by the last dynode ($i = N$). The emission of electrons in the photocathode, as well as the amplification process, are stochastic processes, cf. supplementary material. However, for the sake of clarity, in the following, we just analyze the average behaviour of the PMT using constant and deterministic parameters.

A. Gain

The total gain of a PMT can be expressed [14] as the product

$$G = \eta_{N+1} \prod_{i=1}^{N} g_i, \tag{1}$$

where g_i is the gain of the i-th dynode stage ($i = 1, \ldots, N$), namely the product of the secondary emission coefficient δ_i

Copyright © 2021 IEEE. Personal use is permitted. For any other purposes, permission must be obtained from the IEEE by emailing pubs-permissions@ieee.org.

This is the author's version of an article that has been published in this journal. Changes were made to this version by the publisher prior to publication.
The final version of record is available at http://dx.doi.org/10.1109/JSEN.2021.3062428

and the collection efficiency η_i of the space preceding the dynode $i \in [1, N]$ (which corresponds to n_{i-1} in [14]). η_{N+1} is the anode collection efficiency. The amplification g_i increases exponentially [14, Eq. 1.3] with the inter-electrode voltage $V_i \equiv V(i) - V(i-1)$:

$$g_i = k_i V_i^{\alpha_i}, \tag{2}$$

being $V(i)$ the voltage at electrode i, and α_i and k_i dynode-specific parameters accounting for collection efficiency and secondary emission. α_i and k_i are dimensionless, and the division $V_i/1\,\mathrm{V}$ in the base of the power function has been omitted in the formula for compactness. It should be noted that this simplified mathematical model of the PMT gain is only valid if all $V_i \geq 0\,\mathrm{V}$ for $i = 0, \ldots, N+1$. In general, η_{N+1} depends on the last inter-electrode voltage V_{N+1}. If $V_{N+1} \gg 0\,\mathrm{V}$ is fulfilled, it is usually assumed that the anode collection efficiency $\eta_{N+1} = 1$, and the resulting expression for the gain is independent on V_{N+1}.

In (2), k_i can be replaced with a more general expression depending on a voltage knee parameter $V_{\mathrm{k},i} > 0\,\mathrm{V}$ and the inter-electrode voltage V_i:

$$\tilde{k}_i(V_i) = k_i / \sqrt{1 + V_{\mathrm{k},i}/V_i}, \tag{3}$$

to account for non-linearities in the collection process [1, Eq. 10].

For the simplified case proposed by the commented paper, $\eta_{N+1} = 1$, $\alpha_i = \alpha$ and $k_i = k$ (for $i \in [1, N]$) can be considered constant with voltage and similar for every dynode, see [1, Eq. 4]. Moreover, for the recommended passive resistive network of [1, Fig. 2b] with equal $R_i = 330\,\mathrm{k\Omega}$ for $i \in [1, N]$, in the case of no illumination, the inter-dynode voltages V_i $(i = 1, \ldots, N)$ are a constant (dimensionless) fraction ϵ of the total voltage bias V_B of a high voltage power supply. Hence, (1) and (2) result in:

$$G = \prod_{i=1}^{N} k(\epsilon V_\mathrm{B})^{\alpha} = k^N (\epsilon V_\mathrm{B})^{\alpha N}, \tag{4}$$

again with the implicit division of $V_\mathrm{B}/1\,\mathrm{V}$, and with $\epsilon = 1/(8 + 160/330)$.

B. Electrode currents

Let us define the current $I_{\mathrm{v},i}$ flowing in vacuum from electrode i into electrode $i-1$, with $i = 1, \ldots, N+1$, cf. green arrows in Fig. 1. As the current direction is anti-parallel to the movement of electrons (small blue balls) in the vacuum tube, it follows that $I_{\mathrm{v},i} > 0\,\mathrm{A}$. Following the notation by [1], the magnitude $I_\mathrm{k} > 0\,\mathrm{A}$ of the current emitted by the photocathode is $I_\mathrm{k} = |I_{\mathrm{v},1}|$. The inter-electrode currents in vacuum $I_{\mathrm{v},i}$ yield:

$$I_{\mathrm{v},i} = I_\mathrm{k} \prod_{j=0}^{i-1} g_j \eta_{j+1}, \tag{5}$$

where we introduce $g_0 = 1$ for compactness. The latter equation can be expressed recursively:

$$I_{\mathrm{v},i} = g_{i-1} \eta_i I_{\mathrm{v},i-1}, \tag{6}$$

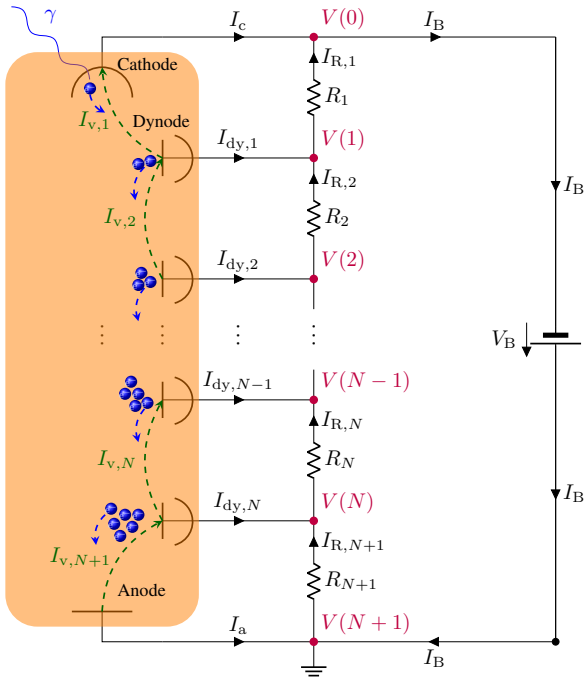

Fig. 1: Schematic of an N-stage PMT connected to a voltage bias V_B in negative polarity mode and a chain of resistors R_i with $i \in [1, N+1]$. The vacuum tube consists of one photocathode ($i = 0$), N dynodes ($i = 1, \ldots, N$), and one anode ($i = N+1$). The electrode voltages $V(i)$ are shown in purple for $i \in [0, N+1]$. The power supply bias current is I_B. The electrode currents are I_c, $I_{\mathrm{dy},i}, i \in [1, N]$, and I_a, whereas the current flowing through the resistors is labeled as $I_{\mathrm{R},i}, i \in [1, N+1]$. A photon ($\gamma$), shown in blue, generates a photoelectron in the cathode. The electrons (small balls) flow in vacuum in the direction of the dashed blue arrow. The dashed green arrows show the sign convention of the definition of the inter-electrode vacuum currents $I_{\mathrm{v},i}$.

by defining $I_{\mathrm{v},0} = I_\mathrm{k}$.

The current $I_{\mathrm{e},i}$ going through each electrode $i = 0, \ldots, N+1$ towards the voltage divider network is obtained using Kirchhoff's current law:

$$I_{\mathrm{e},i} = \begin{cases} I_{\mathrm{v},1} & \text{if } i = 0 \\ I_{\mathrm{v},i+1} - I_{\mathrm{v},i} & \text{if } i = 1, \ldots, N \\ -I_{\mathrm{v},N+1} & \text{if } i = N+1 \end{cases}, \tag{7}$$

where $I_{\mathrm{e},0} \equiv I_\mathrm{c}$, $I_{\mathrm{e},N+1} \equiv I_\mathrm{a}$ and $I_{\mathrm{e},i} \equiv I_{\mathrm{dy},i}$, $i \in [1, N]$, cf. Fig. 1.

For simplicity, it is assumed that electrons emitted by a dynode that are not collected by the next dynode or the anode are deflected back to the emitting dynode (no losses).

Hence, the current flowing into the cathode branch I_c is simply

$$I_\mathrm{c} = I_\mathrm{k} \eta_1. \tag{8}$$

Note that I_k is a parameter in the equations, whereas I_c denotes the current that an ideal ammeter would measure on the cathode.

Copyright © 2021 IEEE. Personal use is permitted. For any other purposes, permission must be obtained from the IEEE by emailing pubs-permissions@ieee.org.

This is the author's version of an article that has been published in this journal. Changes were made to this version by the publisher prior to publication.
The final version of record is available at http://dx.doi.org/10.1109/JSEN.2021.3062428

Using (5), the current flowing into each dynode branch $I_{\mathrm{dy},i}$ is:

$$I_{\mathrm{dy},i} = I_{\mathrm{k}} \left(g_i \eta_{i+1} - 1 \right) \prod_{j=0}^{i-1} g_j \eta_{j+1}, \tag{9}$$

that when all $\eta_i = 1$, $i \in [1, N+1]$ corresponds to [1, Eq. 6].

The current flowing into the anode branch I_{a} yields:

$$I_{\mathrm{a}} = -I_{\mathrm{k}} \prod_{j=0}^{N} g_j \eta_{j+1}, \tag{10}$$

and the gain is:

$$G = -I_{\mathrm{a}} / I_{\mathrm{k}}, \tag{11}$$

according to (1). In the simplified case (4) of constant parameters and all $\eta_i = 1$, the anode current is (assuming very low illumination conditions):

$$I_{\mathrm{a}} = -I_{\mathrm{k}} k^N (\epsilon V_{\mathrm{B}})^{\alpha N}. \tag{12}$$

From (9), if all η_i, $i \in [1, N+1]$ are the unity and k_i, α_i are constants, then the dynode currents yield:

$$I_{\mathrm{dy},i} = I_{\mathrm{k}} k^{i-1} (k V_i^{\alpha} - 1) \prod_{j=0}^{i-1} V_j^{\alpha}, \tag{13}$$

with $V_0 = 1\,\mathrm{V}$ for convenience, and the anode current (10) is:

$$I_{\mathrm{a}} = -I_{\mathrm{k}} k^N \prod_{j=0}^{N} V_j^{\alpha}, \tag{14}$$

where all V_j contain an implicit division of $V_j / 1\,\mathrm{V}$.

In general, the dynode currents $i = 2, \ldots, N$ can be expressed recursively by manipulating (9):

$$I_{\mathrm{dy},i} = I_{\mathrm{dy},i-1} \left(1 - \frac{1}{g_{i-1} \eta_i} \right)^{-1} \left(g_i \eta_{i+1} - 1 \right), \tag{15}$$

which corresponds to [15, Eq 6] when all $\eta_i = 1$, $i \in [1, N+1]$. For the first dynode ($i = 1$), the corresponding equation is:

$$I_{\mathrm{dy},1} = I_{\mathrm{c}} \left(g_1 \eta_2 - 1 \right), \tag{16}$$

which matches [1, Eq. 5] when $\eta_1 = \eta_2 = 1$. For the anode ($i = N+1$), the recursive equation yields:

$$I_{\mathrm{a}} = -I_{\mathrm{dy},N} \left(1 - \frac{1}{g_N \eta_{N+1}} \right)^{-1}. \tag{17}$$

Note that this SPICE modeling of the electrode currents is formally equivalent to the one proposed by [16], where the vacuum currents are simulated in a cascade, which simplifies considerably the expression of the recursion (6) in the current sources compared to (15), and reduces slightly the numerical burden for the solver.

C. Resistive divider network

A common way to supply the $N+2$ electrodes of an N-stage PMT ($N > 0$) is to apply the total voltage bias V_{B} between anode ($i = N+1$, positive) and cathode ($i = 0$, negative), and to use a chain of $N+1$ resistances R_i ($i = 1, \ldots, N+1$) between electrodes i and $i-1$. We define the current I_{B} going from the positive pole of the voltage supply towards the anode, i.e. from the cathode to the negative pole of the source, and $I_{\mathrm{R},i}$ as the current going from electrode i to electrode $i-1$ through resistance R_i. As described before, $V(i)$ are the electrode voltages and $I_{\mathrm{v},i}$ the currents flowing in vacuum from electrode i into electrode $i-1$.

For this passive voltage divider, we ignore the capacitors since we are not modeling the transient response, as well as the small resistive load R_{L} (usually $50\,\Omega$) that is normally connected to the anode when operated in negative polarity. Using Kirchhoff's current law and Ohm's law, the equations governing the PMT model can be formulated as follows for $i = 1, \ldots, N+1$:

$$I_{\mathrm{R},i} + I_{\mathrm{v},i} = I_{\mathrm{B}}, \tag{18}$$

$$V(i) - V(i-1) = I_{\mathrm{R},i} \cdot R_i, \tag{19}$$

$$I_{\mathrm{v},i} = I_{\mathrm{k}} \eta_1 \prod_{j=1}^{i-1} k_j [V(j) - V(j-1)]^{\alpha_j} \eta_{j+1}, \tag{20}$$

where (20) for $i = 1$ is defined instead as just $I_{\mathrm{v},1} = I_{\mathrm{k}} \eta_1$.

Manipulating the equations above, a system of $N+2$ non-linear equations can be defined using the electrode voltages $V(i)$ as variables ($i = 0, \ldots, N+1$):

$$V(0) = -V_{\mathrm{B}}, \tag{21}$$

$$\frac{V(i) - V(i-1)}{R_i} = \frac{V(i+1) - V(i)}{R_{i+1}} + I_{\mathrm{v},i+1} - I_{\mathrm{v},i} \tag{22}$$

$$; \; i \in [1, N], \tag{23}$$

$$V(N+1) = 0. \tag{24}$$

Note that the power supply is connected to ground on the positive pole (anode), i.e. the PMT is operated with negative polarity.

In the case that a voltage booster with bias $V_{\mathrm{b}} > 0\,\mathrm{V}$ is used as in [1, Fig. 6], the system of equations gets modified by the constraint $V(6) = -V_{\mathrm{b}}$, being $V_{\mathrm{b}} < V_{\mathrm{B}}$. As a side note, we have neglected the voltage drop across the $50\,\Omega$ resistors in the referenced divider network.

D. Mathematical model simulation

The behavioral model of the PMT, outlined in Fig. 1, is given by equations (21) through (24), where $N = 8$, $I_{\mathrm{v},i}$ is defined by (20) with $\eta_i = 1$ for $i = 1, \ldots, N+1$, $R_i = 330\,\mathrm{k}\Omega$ for $i = 1, \ldots, N$, $R_{N+1} = 160\,\mathrm{k}\Omega$, $\alpha = 0.881$ and $k = 0.0936$. This system of non-linear equations is solved by applying Newton's method [17], considering the inner node voltages $V(i)$, $i = 1, \ldots, N$ as unknowns. Choosing appropriate starting values for these variables is crucial to get fast convergence. At the beginning, these voltages can be set to the analytical solution of the linear system that results if

Copyright © 2021 IEEE. Personal use is permitted. For any other purposes, permission must be obtained from the IEEE by emailing pubs-permissions@ieee.org.

This is the author's version of an article that has been published in this journal. Changes were made to this version by the publisher prior to publication.
The final version of record is available at http://dx.doi.org/10.1109/JSEN.2021.3062428

TABLE I: Dynode amplification parameters estimated with different methods and resulting PMT gain for three selected voltage bias V_B.

Symbols	Method	G_1	G_2	G_3	Source
	datasheet	$4.75 \cdot 10^2$	$4.93 \cdot 10^5$	$2.34 \cdot 10^6$	Hamamatsu
α_0, k_0	extrapolation	$1.14 \cdot 10^3$	$5.06 \cdot 10^5$	$2.02 \cdot 10^6$	[1]
α, k	optimization	$2.44 \cdot 10^2$	$1.15 \cdot 10^5$	$4.67 \cdot 10^5$	[1]
$\hat{\alpha}$, $\hat{k}$	interpolation	$4.82 \cdot 10^3$	$4.85 \cdot 10^5$	$2.34 \cdot 10^6$	

PMT gain is calculated according to (4) for the passive divider network of [1, Fig. 2b] with $\epsilon = 1/(8 + 160/330)$.
$G_0 \equiv G(300\,\mathrm{V})$, $G_1 \equiv G(800\,\mathrm{V})$, and $G_2 \equiv G(1000\,\mathrm{V})$. The manufacturer gain is extracted graphically from the datasheet with an estimated error of 5 %.
$\alpha_0 \approx 0.7765709$ and $k_0 \approx 0.1512431$; $\alpha \approx 0.7843720$ and $k \approx 0.1213166$; $\hat{\alpha} \approx 0.881$ and $\hat{k} \approx 0.0936$.

$I_k = 0$. Then, we solve non-linear systems for a sequence of parameter values $\{\tilde{I}_k\}$ going from 1 pA to I_k in steps of 1 pA, taking the solution of each system as starting value for the next one. With this strategy, each solution is obtained in at most 3 Newton's method steps, with absolute tolerance 10^{-3}.

Together with this mathematical model, that is solved with MATLAB, we construct the equivalent electrical circuit with the commercial engine PSPICE and the open-source software NGSPICE. Examples of the SPICE circuits are provided in the supplementary materials.

III. Validation

We reproduce the results and Figures of section IV of the commented paper [1] by using two different simulation engines: PSPICE, as the original author, and the open-source NGSPICE. Both engines reported (with our models and parameters) numerically comparable results. Equivalent results were also obtained by solving the analytical equations with MATLAB. No relevant differences were found between the model from [16] and the original one. The SPICE model where the parameters α and k are sampled through auxiliary current sources and resistors for every dynode has been discussed in the supplements.

A. Optimized parameters

Applying [1, Eq. 8] and the initially estimated parameters $\alpha_0 \approx 0.7765709$ and $k_0 \approx 0.1512431$, the manufacturer gain yields $G_1 \equiv G(800\,\mathrm{V}) \approx 5 \cdot 10^5$ and $G_2 \equiv G(1000\,\mathrm{V}) \approx 2 \cdot 10^6$, cf. Table I. The author optimized these parameters so that the result of the PSPICE simulation (compared to the analytical calculation) matched these two data points from the manufacturer gain curve. The simulation sets a very low constant (dark) photocathode current of $I_k = 10\,\mathrm{pA}$ in order to measure the gain via (11). The optimized parameters are $\alpha \approx 0.7843720$ and $k \approx 0.1213166$. However, if one uses [1, Eq. 8] with these new parameters, the result is $G_1 \approx 1.1 \cdot 10^5$ and $G_2 \approx 4.7 \cdot 10^5$, which is inconsistent by more than a factor of 4 with respect to the manufacturer gain, cf. Table I.

To investigate this effect, we recreated the circuit of [1, Fig. 2b] with the SPICE model of [1, Fig. 4], both in the PSPICE and NGSPICE, using a photocathode current I_k of 10 pA. The respective measured anode current I_a at 800 V and 1000 V was $(-1.15 \pm 0.01)\,\mu$A and $(-4.68 \pm 0.02)\,\mu$A for both tools. This matches well with the values G_1 and G_2 calculated analytically using the optimized parameters α and k, and is off by a factor of 4 with respect to the manufacturer gain. On the contrary, if one used instead the initially estimated parameters α_0 and k_0, the measured anode currents would yield $(-5.09 \pm 0.03)\,\mu$A and $(-20.6 \pm 0.05)\,\mu$A, respectively, which match well with the expected gain values.

Presumably, this discrepancy of the optimized parameters might have been caused by an oversight when transcribing the equations of [1] into the SPICE fields, which the optimizer compensates for by returning fairly different parameters so that the gain curve is still matched. For example, the GVALUE of the anode current source (12) might have been written with $N = 9$ in place of $N = 8$. In this hypothetical case, the incorrect ($N = 9$) analytical equation (4) predicts with the optimized parameters gains of $G_1 \approx 4.9 \cdot 10^5$ and $G_2 \approx 2.4 \cdot 10^6$, that match well with the manufacturer gain curve. If this hypothesis were true, one would not be able to reproduce the manufacturer gain curve using these optimized parameters, neither with the true ($N = 8$) analytical gain equation, nor with an independent SPICE model implementation.

Another potential explanation is that the PSPICE simulator default settings are prone to yield numerical errors at low photocathode currents, an effect which is fairly easy to overlook at first. We noticed that the default value of the minimum conductance in every branch $GMIN = 1\,\mathrm{pA}$ had to be overwritten with 1 fA or lower to get a reliable current source simulation. More details are given in Fig. S1 of the supplementary materials.

However, it is true that one can not stay with the initially estimated parameters α_0 and k_0 by extrapolating them for voltages below 800 V, as the predicted gain with $N = 8$ at 300 V would yield $G_0 \equiv G(300\,\mathrm{V}) \approx 1.1 \cdot 10^3$, higher than the manufacturer value of $\approx 4.8 \cdot 10^2$, cf. Table I. If we use the wrong gain equation with $N = 9$ and the optimized parameters, the result matches better $\approx 4.8 \cdot 10^2$. Hence, one must recalculate the parameters α and k, as the initial estimate provided in [1] only works well in the area between 800 V and 1000 V, whereas the optimized ones suffer from a likely error in the SPICE model.

Our approach is not to use an optimizer, but just two accurate values of the manufacturer curve, one at each end, so that no extrapolation error appears. This is legitimate, as the manufacturer gain is a straight line in a double-logarithmic plot, cf. [1, Fig. 2a], and thus there is no interpolation error. We import the manufacturer datasheet (PDF) in an open-source Scalable Vector Graphics (SVG) editor [18] and read out the pixel coordinates of the line, as well as of the axis. The resulting formula is

$$G(V_B) = 10^{(-14.77 \pm 0.01)} \cdot V_B^{(7.048 \pm 0.001)}, \qquad (25)$$

where $V_B > 0\,\mathrm{V}$ is the power supply voltage (magnitude) applied to the standard divider network recommended by the vendor, see [1, Fig. 2b]. It contains eight resistances of 330 kΩ and one of 160 kΩ between the anode and the last dynode. The base of the power function contains an implicit division

Copyright © 2021 IEEE. Personal use is permitted. For any other purposes, permission must be obtained from the IEEE by emailing pubs-permissions@ieee.org.

This is the author's version of an article that has been published in this journal. Changes were made to this version by the publisher prior to publication.
The final version of record is available at http://dx.doi.org/10.1109/JSEN.2021.3062428

of $V_\mathrm{B}/1\,\mathrm{V}$. We estimate that the reconstructed manufacturer gain curve (25) is accurate with a $5\,\%$ error margin.

Combining (25) and (4) with $\epsilon_i = 1/(8 + 160/330) \approx 0.1179$ ($\approx 1/8.5$) for $i = 1, \ldots, 8$, we obtain a faithful value of $\hat{\alpha} = (0.881 \pm 0.001)$ and $\hat{k} = (0.0936 \pm 0.0002)$. The resulting gains with these parameters are $\hat{G}_0 \approx (4.82 \pm 0.05) \cdot 10^2$, $\hat{G}_1 \approx (4.85 \pm 0.05) \cdot 10^5$, and $\hat{G}_2 \approx (2.34 \pm 0.04) \cdot 10^6$, cf. Table I.

When simulating the circuit both in PSPICE and NGSPICE with these parameters and $I_\mathrm{k} = 1\,\mathrm{pA}$, compatible gain values are measured. The numerical solution with MATLAB matches, too. If the simulation is performed instead with $I_\mathrm{k} = 10\,\mathrm{pA}$, the resulting gain is slightly off by $4\,\%$ with respect to the analytical calculation.

B. Gain over voltage bias

In Fig. 2a, we reproduce the PMT gain over voltage curves of a passive divider network [1, Fig. 2b] for different photocathode currents, cf. [1, Fig. 5] of the commented paper, but with the graphically derived parameters $\hat{\alpha}$ and $\hat{k}$. Our results are self-consistent, as NGSPICE, PSPICE and MATLAB report nearly identical results, but are not compliant with [1, Fig. 5], whose data points are depicted as colored circles in our Figure.

A potential reason for this discrepancy might be an incorrect sign of I_k in the author's SPICE simulation (for this Figure). To test this hypothesis, we recalculate Fig. 2a (for $\hat{\alpha} = 0.881$ and $\hat{k} = 0.0936$) with a negative sign of I_k and obtain curves, cf. Fig. 2b, that match now moderately well with the colored circles, namely the data points extracted from [1, Fig. 5] using $\alpha = 0.7843720$ and $k = 0.1213166$.

Our hypothesis of a flipped sign affecting [1, Fig. 5] (but not further figures within that manuscript) is sustained by the good agreement of Fig. 2b as well as by a later publication of the same author [2, Fig. 4 and 5a], where results similar to our Figs. 2a and 5a are obtained.

C. Inter-dynode voltages

In Fig. 3, we reproduce the PMT voltage stability using a resistive divider network with a fixed -100 V booster [1, Fig. 6], as done in [1, Fig. 7]. We depict the variation in inter-dynode voltage V_i ($i = 1, \ldots, 8$) with no incident light (dark current of $I_\mathrm{k} = 10\,\mathrm{pA}$) compared to maximum illumination (a photocathode current I_k such that $I_\mathrm{a} \approx -400\,\mu\mathrm{A}$). The simulated results (with $\hat{\alpha} = 0.881$ and $\hat{k} = 0.0936$) match moderately well with the experimental data points of [5, Fig. 13], and show a similar trend than those from [1, Fig. 7] (with $\alpha = 0.7843720$ and $k = 0.1213166$), which have not been depicted here.

D. Gain non-linearity

In Fig. 4, we reproduce the PMT gain stability using the aforementioned divider network with booster [1, Fig. 6], as done in [1, Fig. 8]. We depict the variation in gain G with no incident light (dark current of $I_\mathrm{k} = 10\,\mathrm{pA}$) compared to maximum illumination (a photocathode current I_k such that

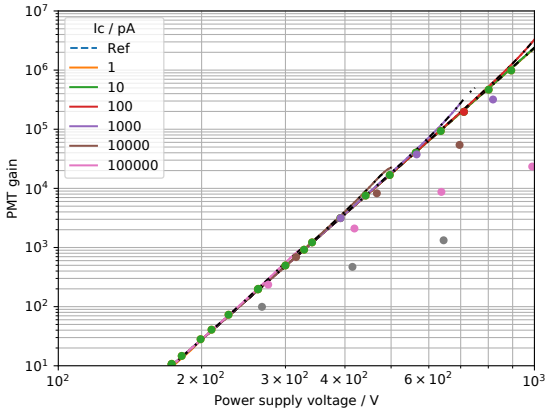

(a) Correct sign of photocathode current. Note that the curves with high photocathode currents are stopped at earlier voltages due to convergence problems when the standing bias current is comparable to the amplified current. The case with $1\,\mu\mathrm{A}$ did not converge either and was left out.

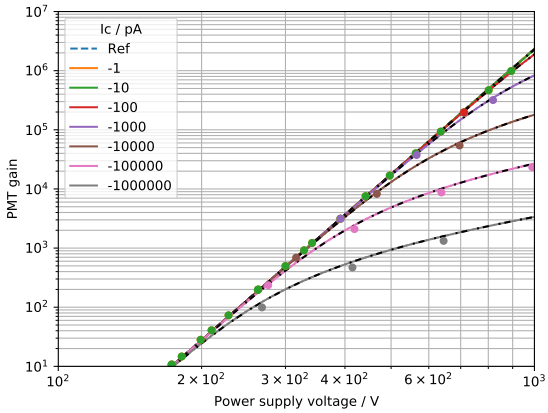

(b) Flipped sign of photocathode current. Note that an artificial negative sign on parameter I_k was introduced in all equations.

Fig. 2: PMT gain G of a passive divider network [1, Fig. 2] measured with an NGSPICE simulation using (11) for $\hat{\alpha} = 0.881$ and $\hat{k} = 0.0936$, as a function of the power supply voltage V_B for different values of the photocathode current I_c. The blue dashed curve represents the manufacturer gain (25). The solid curves are the simulation results, and the superimposed dotted lines with the same color are the results obtained with PSPICE. The calculations with MATLAB are visible as black dash-dotted lines. The solid circles of matching colors correspond to data points extracted graphically from [1, Fig. 5], which used $\alpha = 0.7843720$ and $k = 0.1213166$.

Copyright © 2021 IEEE. Personal use is permitted. For any other purposes, permission must be obtained from the IEEE by emailing pubs-permissions@ieee.org.

This is the author's version of an article that has been published in this journal. Changes were made to this version by the publisher prior to publication.
The final version of record is available at http://dx.doi.org/10.1109/JSEN.2021.3062428

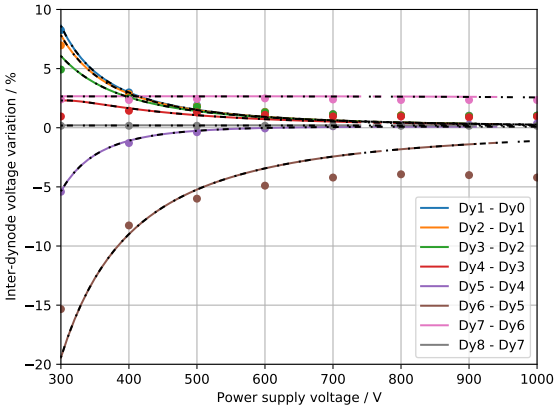

Fig. 3: Relative variation of the inter-dynode voltage $V_{i,\mathrm{bright}}/V_{i,\mathrm{dark}} - 1$ for a passive+booster network [1, Fig. 6] with no illumination $V_{i,\mathrm{dark}} \equiv V_i(I_\mathrm{k} = 10\,\mathrm{pA})$ compared to maximum illumination $V_{i,\mathrm{bright}} \equiv V_i(I_\mathrm{k}(I_\mathrm{a} = -400\,\mu\mathrm{A}))$, as a function of the total power supply voltage V_B (keeping the booster voltage fixed). The solid curves depict the voltage variations measured with the NGSPICE simulation for $\hat{\alpha} = 0.881$ and $\hat{k} = 0.0936$, and the black dash-dotted lines depict the corresponding results with MATLAB. The solid circles correspond to experimental measurements extracted graphically from [5, Fig. 13].

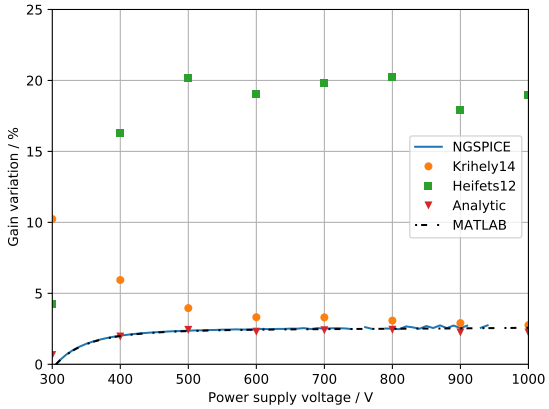

Fig. 4: Relative variation of the PMT gain $G_{\mathrm{bright}}/G_{\mathrm{dark}} - 1$ for a passive+booster network [1, Fig. 6] with no illumination $G_{\mathrm{dark}} \equiv G(I_\mathrm{k} = 10\,\mathrm{pA})$ compared to maximum illumination $G_{\mathrm{bright}} \equiv G(I_\mathrm{k}(I_\mathrm{a} = -400\,\mu\mathrm{A}))$, as a function of the total power supply voltage V_B (keeping the booster voltage fixed). The blue solid curve depicts the gain variation measured with the NGSPICE simulation for $\hat{\alpha} = 0.881$ and $\hat{k} = 0.0936$, and the black dash-dotted line depicts the corresponding result with MATLAB. The orange circles correspond to the simulation of [1, Fig. 8] obtained with $\alpha = 0.7843720$ and $k = 0.1213166$. The green squares are the experimental measurements extracted graphically from [5, Fig. 15]. The red triangles represent the analytical prediction (27) using the experimental values of ϕ_i from [5, Fig. 13].

$I_\mathrm{a} \approx -400\,\mu\mathrm{A}$). The simulated results (with $\hat{\alpha} = 0.881$ and $\hat{k} = 0.0936$) do not match with those of [1, Fig. 8] (with $\alpha = 0.7843720$ and $k = 0.1213166$), nor with the experimental data points of [5, Fig. 15].

This discrepancy is mentioned in [1] and attributed to experimental measurement errors in [5]. To verify the theoretical inconsistency of Figs. 13 and 15 of [5], we calculate analytically what the expected gain variation would be, cf. red triangles of Fig. 4. This is performed using the experimentally measured inter-dynode voltage variations, which seem to match more faithfully with the simulation, cf. Fig. 3. Using (1) and (2) for a constant k, the gain $G(I_\mathrm{k})$ is:

$$G(I_\mathrm{k}) = k^N \prod_{i=1}^{N} \left(V_i(I_\mathrm{k})\right)^\alpha \tag{26}$$

and the relative variation when using a different photocathode current $\tilde{I}_\mathrm{k}$ yields:

$$\frac{G(\tilde{I}_\mathrm{k})}{G(I_\mathrm{k})} - 1 = -1 + \prod_{i=1}^{N} \left(\frac{V_i(\tilde{I}_\mathrm{k})}{V_i(I_\mathrm{k})}\right)^\alpha = -1 + \prod_{i=1}^{N} (\phi_i + 1)^\alpha, \tag{27}$$

where the terms $\phi_i \equiv V_i(\tilde{I}_\mathrm{k})/V_i(I_\mathrm{k}) - 1$ are the data points presented in Fig. 3.

The mismatch between gain variation measurement and simulations might be due to experimental uncertainties, or because the SPICE model is not sophisticated enough and does not account for the anode collection efficiency, as well as dynode-specific effects and non-linearities. Nonetheless, the analytic prediction of the gain variation using experimental voltage measurements [5, Fig. 13] matches remarkably well with the NGSPICE simulation results, cf. Fig. 4, using our parameters $\hat{\alpha}$ and $\hat{k}$.

E. Anode collection efficiency

When operated at a voltage bias V_B of 1000 V, the SPICE model under investigation predicts, cf. Fig. 5a, first an increase of the gain with the amount of incident light and then a decrease above a photocathode current of 175 pA. This complies with the observation from [2, Fig. 5a]. Furthermore, the inter-dynode voltages, cf. Fig. 6a follow a similar trend than those of [2, Fig. 6a].

The results presented here are valid mathematical solutions of the PMT model under investigation, however they do not describe faithfully the physical behaviour of the PMT at photocathode currents above 100 pA. The reason is that the PMT model assumes that the anode collection efficiency $\eta_{N+1} \approx 1$ under the condition that the $V_{N+1} \gg 0$ V. However, the premise that the voltage between anode and last dynode is large enough does not hold in the examples above, as it is shown in cf. Fig. 7a. Above 100 pA, the voltage at the last dynode is above the voltage at the anode, i.e. $V_{N+1} < 0$ V. Under this condition, the anode would not collect any electron emitted by the last dynode; it would rather deflect them back to the dynode, hence $\eta_{N+1} \to 0$.

We propose an ad-hoc model of the voltage-dependent anode collection efficiency $\eta_{N+1}(V_{N+1})$ using the logistic

Copyright © 2021 IEEE. Personal use is permitted. For any other purposes, permission must be obtained from the IEEE by emailing pubs-permissions@ieee.org.

This is the author's version of an article that has been published in this journal. Changes were made to this version by the publisher prior to publication.
The final version of record is available at http://dx.doi.org/10.1109/JSEN.2021.3062428

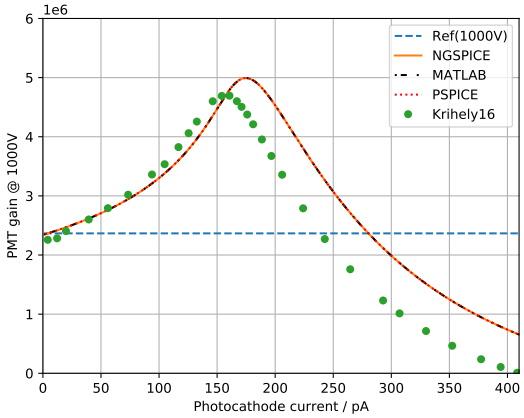

(a) Ideal anode collection efficiency. The green circles are data points derived graphically from [2, Fig. 5a], that used $\alpha = 0.7843720$ and $k = 0.1213166$.

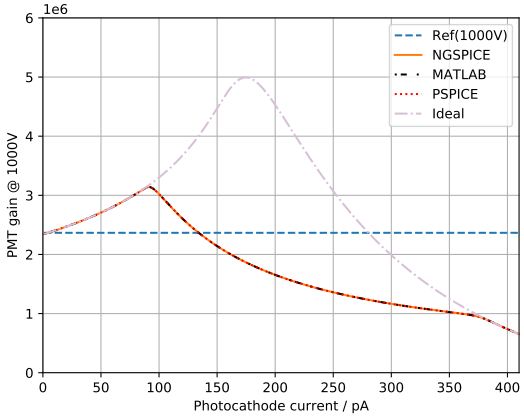

(b) Realistic formula for the anode collection efficiency (28). For comparison, the MATLAB result with ideal efficiency is shown as a thistle dash-dotted line.

Fig. 5: PMT gain G of a passive divider network [1, Fig. 2b] as a function of photocathode current I_c for a fixed power supply voltage $V_B = 1000\,\mathrm{V}$. The blue dashed line depicts the gain according to the manufacturer, and the solid orange curve is the one measured with the NGSPICE simulation for $\hat{\alpha} = 0.881$ and $\hat{k} = 0.0936$. The PSPICE curve is depicted with red dots and the MATLAB result is shown as a black dash-dotted line.

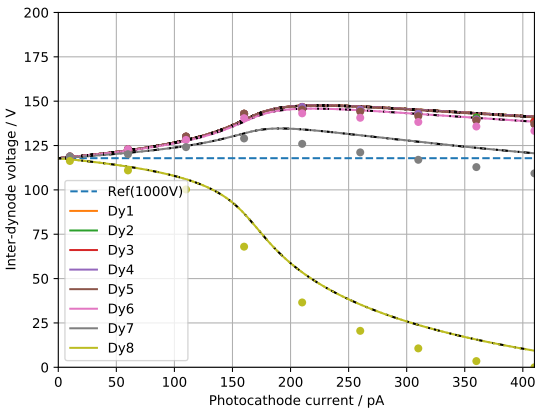

(a) Ideal anode collection efficiency. The colored circles are data points derived graphically for each dynode from [2, Fig. 6a], that used $\alpha = 0.7843720$ and $k = 0.1213166$.

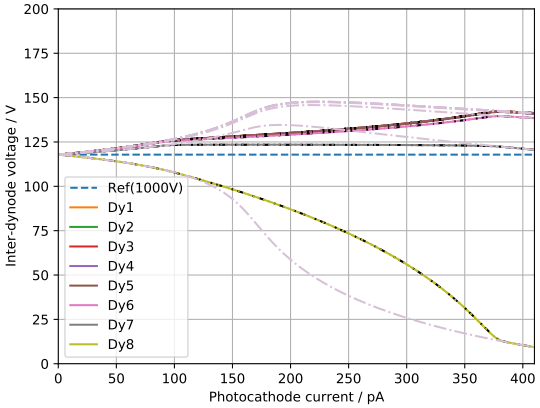

(b) Realistic formula for the anode collection efficiency (28). For comparison, the MATLAB result with ideal efficiency is shown as thistle dash-dotted lines.

Fig. 6: Inter-dynode voltage $V_i \equiv V(i) - V(i-1)$, $i \in [1, N]$ of a passive divider network [1, Fig. 2b] as a function of photocathode current I_c for a fixed power supply voltage $V_B = 1000\,\mathrm{V}$. The blue dashed line depicts the nominal inter-dynode voltage according to the divider network (under no light), and the solid orange curve is the one measured with the NGSPICE simulation for $\hat{\alpha} = 0.881$ and $\hat{k} = 0.0936$. The colored dotted lines are the corresponding simulations with PSPICE and the MATLAB results are shown as black dash-dotted lines.

function:

$$\eta_{N+1}(V_{N+1}) = \frac{1}{1 + \exp\left[(10\,\mathrm{V} - V_{N+1})/1\,\mathrm{V}\right]}, \tag{28}$$

that is 1 for $V_{N+1} \gg 10\,\mathrm{V}$ and tends to zero when $V_{N+1} \ll 10\,\mathrm{V}$.

Thus, the SPICE model equations have to be modified for the last dynode (15) and the anode (17) substituting (28) for η_{N+1}. The corresponding results are shown in Figs. 5b, 6b and 7b. Whereas the logistic model for the anode collection efficiency is over-simplistic and the knee parameter of 10 V arbitrary, it shows that the results are more realistic from the physical point of view, as the voltage of the last dynode never surpasses in this case the anode voltage.

IV. Conclusion

In our comment, we have revisited and disambiguated the mathematical formulation of the behavioral SPICE model of a PMT [1]. We have also addressed some inconsistencies in the optimized parameters as well as a presumable oversight in a sign affecting one of the original Figures.

Furthermore, we have shown that the original SPICE model predicts in some situations positive voltages at the last two dynodes, which is not realistic from the physical point of

Copyright © 2021 IEEE. Personal use is permitted. For any other purposes, permission must be obtained from the IEEE by emailing pubs-permissions@ieee.org.

This is the author's version of an article that has been published in this journal. Changes were made to this version by the publisher prior to publication.
The final version of record is available at http://dx.doi.org/10.1109/JSEN.2021.3062428

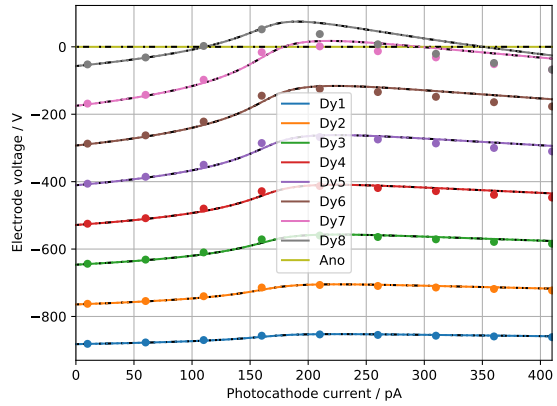

(a) Ideal anode collection efficiency. The colored circles are data points derived graphically for each dynode from [2, Fig. 6a], that used $\alpha = 0.7843720$ and $k = 0.1213166$.

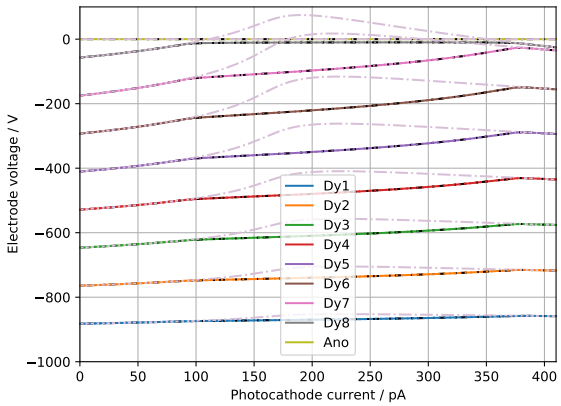

(b) Realistic formula for the anode collection efficiency (28). For comparison, the MATLAB result with ideal efficiency is shown as thistle dash-dotted lines.

Fig. 7: Electrode voltages $V(i)$ of a passive divider network [1, Fig. 2b] as a function of photocathode current I_c for a fixed power supply voltage $V_B = 1000\,\text{V}$. The solid curves are the voltages measured with the NGSPICE simulation for $\hat{\alpha} = 0.881$ and $\hat{k} = 0.0936$. The colored dotted lines are the corresponding simulations with PSPICE and the MATLAB results are shown as black dash-dotted lines.

view. This effect can be mitigated by introducing a term in the equations in order to model the anode collection efficiency.

All SPICE simulations have been replicated with corrected parameters using both NGSPICE and PSPICE, and the results were in accordance with the numerical solution of the system of non-linear equations using Newton's method in MATLAB.

Acknowledgment

F. Hueso-González thanks N. Krihely for discussion and clarifications about his manuscript, as well as Clyde, M. Hendrix, H. Vogt and D. Warning from the NGSPICE community on Sourceforge for excellent support.

References

[1] Krihely N. SPICE Model of Photomultiplier Tube Under Different Bias Conditions. IEEE Sensors Journal. 2014;14(10):3606–3610. Available from: https://doi.org/10.1109/JSEN.2014.2329181.

[2] Krihely N. Comparing passive and active biasing networks for a photomultiplier tube sensor using SPICE. In: 2016 IEEE International Conference on the Science of Electrical Engineering (ICSEE); 2016. p. 1–5. Available from: https://doi.org/10.1109/ICSEE.2016.7806182.

[3] Lush HJ. Photomultiplier linearity. J Sci Instrum. 1965;42(8):597–602. Available from: https://doi.org/10.1088/0950-7671/42/8/328.

[4] Land PL. A Discussion of the Region of Linear Operation of Photomultipliers. Rev Sci Instrum. 1971;42(4):420–425. Available from: https://doi.org/10.1063/1.1685117.

[5] Heifets M, Margulis P. Fully active voltage divider for PMT photodetector. In: IEEE Nucl Sci Symp Conf Rec; 2012. p. 807–814. Available from: https://doi.org/10.1109/NSSMIC.2012.6551216.

[6] Pausch G, Berthold J, Enghardt W, Roemer K, Straessner A, Wagner A, et al. Detection systems for range monitoring in proton therapy: Needs and challenges. Nucl Instr Methods Phys Res A. 2018;Available from: https://doi.org/10.1016/j.nima.2018.09.062.

[7] Hueso-González F, Bortfeld T. Compact Method for Proton Range Verification Based on Coaxial Prompt Gamma-Ray Monitoring: a Theoretical Study. IEEE Trans Radiat Plasma Med Sci. 2020;4(2):170–183. Available from: https://doi.org/10.1109/TRPMS.2019.2930362.

[8] Werner T, Berthold J, Hueso-González F, Petzoldt J, Roemer K, Richter C, et al. Processing of prompt gamma-ray timing data for proton range measurements at a clinical beam delivery. Phys Med Biol. 2019;1(10):105023. Available from: https://doi.org/10.1088/1361-6560/ab176d.

[9] Lannutti F, Menichelli F, Nenzi P, Olivieri M. A new algorithm for convergence verification in circuit level simulations. In: 2014 10th Conference on Ph.D. Research in Microelectronics and Electronics (PRIME); 2014. p. 1–4. Available from: https://doi.org/10.1109/PRIME.2014.6872721.

[10] Conant R. Engineering Circuit Analysis with PSpice and Probe. USA: McGraw-Hill, Inc.; 1993. Available from: https://dl.acm.org/doi/book/10.5555/541728.

[11] MATLAB 9.7.0.1190202 (R2019b). Natick, Massachusetts: The MathWorks Inc.; 2018. Available from: https://es.mathworks.com/products/matlab.html.

[12] Lubsandorzhiev BK. On the history of photomultiplier tube invention. Nucl Instr Methods Phys Res A. 2006;567(1):236–238. Available from: https://doi.org/10.1016/j.nima.2006.05.221.

[13] Zaghloul ME, Rhee DJ. Computer-aided simulation study of photomultiplier tubes. IEEE Trans Electron Devices. 1989;36(9):2005–2010. Available from: https://doi.org/10.1109/16.34284.

[14] Flyckt SO, Marmonier C. Photomultiplier tubes: principles and applications; 2nd ed. Brive-la-Gaillarde, France: Photonis; 2002. Available from: http://www2.pv.infn.it/~debari/doc/Flyckt_Marmonier.pdf.

[15] Akimov DY, Kozlova ES, Melikyan YA. Computer modelling of the Hamamatsu R11410-20 PMT. Journal of Physics: Conference Series. 2017;798:012211. Available from: https://doi.org/10.1088/1742-6596/778/1/012211.

[16] Peña Rodríguez J, Hernández-Barajas S, León-Carreño Y, Núñez LA. Modeling and simulation of the R5912 photomultiplier for the LAGO project. IEEE Sens J. 2021;Available from: https://doi.org/10.1109/JSEN.2021.3096426.

[17] Ypma TJ. Historical development of the Newton–Raphson method. SIAM review. 1995;37(4):531–551. Available from: http://www.jstor.org/stable/2132904.

[18] Inkscape 0.92.5; 2020. Available from: https://inkscape.org.

Copyright © 2021 IEEE. Personal use is permitted. For any other purposes, permission must be obtained from the IEEE by emailing pubs-permissions@ieee.org.

This is the author's version of an article that has been published in this journal. Changes were made to this version by the publisher prior to publication.
The final version of record is available at http://dx.doi.org/10.1109/JSEN.2021.3062428

SUPPLEMENTARY MATERIAL

NGSPICE circuit file

Listing 1: NGSPICE circuit file of a PMT using the recursive formulation, cf. (15), (16), and (17), for reproducing Figs. 5a, 6a and 7a.

```
*  NODE NUMBERS
*                           Dynode 1
*                           |   Dynode 2
*                           |   |   Dynode 3
*                           |   |   |   Dynode 4
*                           |   |   |   |   Dynode 5
*                           |   |   |   |   |   Dynode 6
*                           |   |   |   |   |   |   Dynode 7
*                           |   |   |   |   |   |   |   Dynode 8
*                           |   |   |   |   |   |   |   |   Cathode
*                           |   |   |   |   |   |   |   |   |   Anode
*                           |   |   |   |   |   |   |   |   |   |   Cathode current plus
*                           |   |   |   |   |   |   |   |   |   |   |    Cathode current minus
*                           |   |   |   |   |   |   |   |   |   |   |    |
.SUBCKT KRIHELY14_Dyn08     Dy1 Dy2 Dy3 Dy4 Dy5 Dy6 Dy7 Dy8 Cat Ano Scp  Scm    PARAMS: alpha=0.78 k=0.12
* alpha: dynode-specific parameter
* k: dynode-specific parameter
* N. Krihely, "SPICE Model of Photomultiplier Tube Under Different Bias Conditions,"
* in IEEE Sensors Journal, vol. 14, no. 10, pp. 3606-3610, Oct. 2014, doi: 10.1109/JSEN.2014.2329181.
* https://doi.org/10.1109/JSEN.2014.2329181

* Amplification functions
.func gvald(ip, alpha, k, v, vp     ) = { ip *( k * (v-vp)**alpha - 1)                                  }
.func gval (ip, alpha, k, v, vp, vpp) = { ip *( k * (v-vp)**alpha - 1) / ( 1 - 1 / ( k * (vp-vpp)**alpha)) }
.func gvala(ip, alpha, k, v, vp, vpp) = { ip                         / ( 1 - 1 / ( k * (vp-vpp)**alpha)) }

* Measure photocathode current
VMES0 Scm Cat 0
R0 Scp GND 0

* Measure stage currents
VMES1  SDy1 Dy1 0
VMES2  SDy2 Dy2 0
VMES3  SDy3 Dy3 0
VMES4  SDy4 Dy4 0
VMES5  SDy5 Dy5 0
VMES6  SDy6 Dy6 0
VMES7  SDy7 Dy7 0
VMES8  SDy8 Dy8 0
VMES20 SAno Ano 0

* Dynode amplification stages
G1  GND SDy1 GND GND value= gvald( I(VMES0), {alpha}, {k}, V(Dy1), V(Cat)         )
G2  GND SDy2 GND GND value= gval(  I(VMES1), {alpha}, {k}, V(Dy2), V(Dy1), V(Cat) )
G3  GND SDy3 GND GND value= gval(  I(VMES2), {alpha}, {k}, V(Dy3), V(Dy2), V(Dy1) )
G4  GND SDy4 GND GND value= gval(  I(VMES3), {alpha}, {k}, V(Dy4), V(Dy3), V(Dy2) )
G5  GND SDy5 GND GND value= gval(  I(VMES4), {alpha}, {k}, V(Dy5), V(Dy4), V(Dy3) )
G6  GND SDy6 GND GND value= gval(  I(VMES5), {alpha}, {k}, V(Dy6), V(Dy5), V(Dy4) )
G7  GND SDy7 GND GND value= gval(  I(VMES6), {alpha}, {k}, V(Dy7), V(Dy6), V(Dy5) )
G8  GND SDy8 GND GND value= gval(  I(VMES7), {alpha}, {k}, V(Dy8), V(Dy7), V(Dy6) )
G20 SAno GND GND GND value= gvala( I(VMES8), {alpha}, {k}, V(Ano), V(Dy8), V(Dy7) )

.ENDS
*-------------------------------------------------------------------------------

* Divider network for R7400U, corresponding to Fig.2b of Krihely2014

* Total voltage bias
V0 GND Cathode 1000

* Photocathode current
I0 Sinp Sinm dc 1p

* PMT subcircuit connection
XPMT1 d1 d2 d3 d4 d5 d6 d7 d8 Cathode GND Sinp Sinm KRIHELY14_Dyn08 PARAMS: alpha=0.881 k=0.0936

* Passive divider network
R1 Cathode d1 330k
R2 d1 d2 330k
R3 d2 d3 330k
R4 d3 d4 330k
R5 d4 d5 330k
R6 d5 d6 330k
R7 d6 d7 330k
R8 d7 d8 330k
R9 d8 GND 160k

* Condensators
C1 d7 d6 10n
```

Copyright © 2021 IEEE. Personal use is permitted. For any other purposes, permission must be obtained from the IEEE by emailing pubs-permissions@ieee.org.

This is the author's version of an article that has been published in this journal. Changes were made to this version by the publisher prior to publication.
The final version of record is available at http://dx.doi.org/10.1109/JSEN.2021.3062428


```
C2 d8 d7 10n
C3 d8 GND 10n

* DC Sweep
.dc I0 1p 400p 1p

* Control and Plots
.control
version
run
display
plot -v.xpmt1.vmes20#branch/v.xpmt1.vmes0#branch
plot d2-d1 d3-d2 d4-d3 d5-d4 d6-d5 d7-d6 d8-d7
plot d1 d2 d3 d4 d5 d6 d7 d8 xpmt1.sano
.endc

.end
```

Numerical error amplification in PSPICE

If a circuit similar to Listing 1 is implemented in PSPICE using the default solver settings, there is a critical amplification of numerical errors that leads to senseless simulation results. This is because the default value of the minimum conductance $GMIN$ of every branch in PSPICE yields 1 pA per volt, e.g. the voltage drop across the two nodes of a current source. In the case of 1000 V total voltage bias, the current source representing the photocathode inyects an error of 1000 pA, which can be comparable or higher than the illumination conditions under study. If the source current is measured with an ammeter, there will be a significant numerical error that is amplified in further stages.

This numerical error is illustrated in Fig. S1 for the PSPICE circuit outlined in Listing 2. It should be noted that the simulated gain has been measured as the quotient between the current measured with a dummy voltage source (0 V), acting as an ideal ammeter, on the anode versus the cathode branch. If one would use the real value of I_k in the denominator, the error would be much larger, especially for low photocathode currents.

If the author used some recursivity in the equations as the presence of sensing 0 V voltage sources in [1, Fig. 3] seems to hint at, there is a possibility that this effect might was overlooked. Then, the simulated gain at the photocathode current of 10 pA used for his simulation would be overestimated, as shown in Fig. S1, and reducing the amplification parameters k_0 and α_0 towards k and α, cf. Table I, during the optimization step could have compensated for it. Leading also to an overall bias and a discrepancy with the proposed equations.

Hence, the solution to prevent this potential error is to change the value $GMIN$ from 10^{-12} to e.g. 10^{-18}, or to leave the default value of $GMIN$ and use instead the explicit formulation, cf. Listing 3. In the latter case, there is still some error in the current of the cathode branch, but the error is not amplified by subsequent dynodes as the behavioral source equations use the original parameter I_k.

Listing 2: PSPICE netlist file of a PMT using the recursive formulation, cf. (16), (15), and (17).

```
** Analysis setup **
.PARAM         Ik=10pA al=0.881 k=0.0936
.DC LIN PARAM Ik 1p 400p 1p
.OPTIONS GMIN=0.001f

* Passive divider network
R_R1          A2 A1  330k
R_R2          A3 A2  330k
R_R3          A4 A3  330k
R_R4          A5 A4  330k
R_R5          A6 A5  330k
R_R6          A7 A6  330k
R_R7          A8 A7  330k
R_R8          A9 A8  330k
R_R9          0 A9  160k

* Measure stage currents
V_V10          Cat A1 DC 0
V_V11          Dy1 A2 DC 0
V_V12          Dy2 A3 DC 0
V_V13          Dy3 A4 DC 0
V_V14          Dy4 A5 DC 0
V_V15          Dy5 A6 DC 0
V_V16          Dy6 A7 DC 0
V_V17          Dy7 A8 DC 0
V_V18          Dy8 A9 DC 0

* Amplification functions
G_G1          0 Dy1 VALUE { I(V_V10)*(k*V(A2,A1)**al-1) }
G_G2          0 Dy2 VALUE { I(V_V11)/(1-1/(k*V(A2,A1)**al))*(k*V(A3,A2)**al-1) }
G_G3          0 Dy3 VALUE { I(V_V12)/(1-1/(k*V(A3,A2)**al))*(k*V(A4,A3)**al-1) }
G_G4          0 Dy4 VALUE { I(V_V13)/(1-1/(k*V(A4,A3)**al))*(k*V(A5,A4)**al-1) }
G_G5          0 Dy5 VALUE { I(V_V14)/(1-1/(k*V(A5,A4)**al))*(k*V(A6,A5)**al-1) }
G_G6          0 Dy6 VALUE { I(V_V15)/(1-1/(k*V(A6,A5)**al))*(k*V(A7,A6)**al-1) }
G_G7          0 Dy7 VALUE { I(V_V16)/(1-1/(k*V(A7,A6)**al))*(k*V(A8,A7)**al-1) }
```

Copyright © 2021 IEEE. Personal use is permitted. For any other purposes, permission must be obtained from the IEEE by emailing pubs-permissions@ieee.org.

This is the author's version of an article that has been published in this journal. Changes were made to this version by the publisher prior to publication.
The final version of record is available at http://dx.doi.org/10.1109/JSEN.2021.3062428

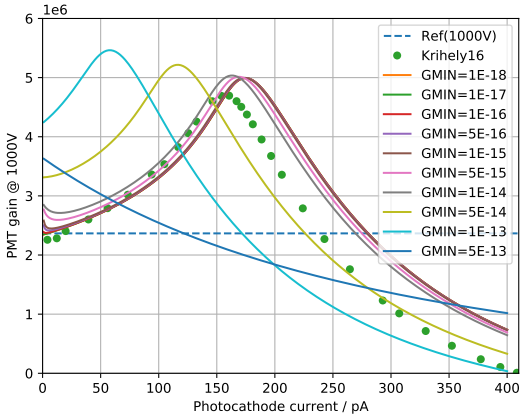

Fig. S1: PMT gain G of a passive divider network [1, Fig. 2b] as a function of photocathode current I_c for a fixed power supply voltage $V_B = 1000\,V$. The blue dashed line depicts the gain according to the manufacturer, and the solid curves are the ones measured with the PSPICE simulation, cf. Listing 3, for $\hat{\alpha} = 0.881$ and $\hat{k} = 0.0936$, for different values of $GMIN$. The green circles are data points derived graphically from [2, Fig. 5a], that used $\alpha = 0.7843720$ and $k = 0.1213166$.

```
G_G8          0 Dy8 VALUE { I(V_V17)/(1-1/(k*V(A8,A7)**al))*(k*V(A9,A8)**al-1) }
G_G9          0 0 VALUE   {-I(V_V18)/(1-1/(k*V(A9,A8)**al)) }

* Supply
V_V1          0 A1 1000V
I_I1          0 Cat DC {Ik}

.END
```

Listing 3: PSPICE netlist file of a PMT using the explicit formulation, cf. (9), and (10).

```
** Analysis setup **
.PARAM          Ik=10pA al=0.881 k=0.0936
.DC LIN PARAM Ik 1p 400p 1p

* Passive divider network
R_R1          A2 A1  330k
R_R2          A3 A2  330k
R_R3          A4 A3  330k
R_R4          A5 A4  330k
R_R5          A6 A5  330k
R_R6          A7 A6  330k
R_R7          A8 A7  330k
R_R8          A9 A8  330k
R_R9          0 A9  160k

* Amplification functions
G_G1          0 A2 VALUE { Ik*(k*V(A2,A1)**al-1) }
G_G2          0 A3 VALUE { Ik*k*(V(A2,A1)**al)*(k*V(A3,A2)**al-1) }
G_G3          0 A4 VALUE { Ik*k**2*((V(A2,A1)*V(A3,A2))**al)*(k*V(A4,A3)**al-1)
+  }
G_G4          0 A5 VALUE {
+  Ik*k**3*((V(A2,A1)*V(A3,A2)*V(A4,A3))**al)*(k*V(A5,A4)**al-1) }
G_G5          0 A6 VALUE {
+  Ik*k**4*((V(A2,A1)*V(A3,A2)*V(A4,A3)*V(A5,A4))**al)*(k*V(A6,A5)**al-1) }
G_G6          0 A7 VALUE {
+  Ik*k**5*((V(A2,A1)*V(A3,A2)*V(A4,A3)*V(A5,A4)*V(A6,A5))**al)*(k*V(A7,A6)**al-1)
+  }
G_G7          0 A8 VALUE {
+  Ik*k**6*((V(A2,A1)*V(A3,A2)*V(A4,A3)*V(A5,A4)*V(A6,A5)*V(A7,A6))**al)*(k*V(A8,A7)**al-1)
+  }
G_G8          0 A9 VALUE {
+  Ik*k**7*((V(A2,A1)*V(A3,A2)*V(A4,A3)*V(A5,A4)*V(A6,A5)*V(A7,A6)*V(A8,A7))**al)*(k*V(A9,A8)**al-1)
+  }
G_G9          0 0 VALUE {
+  -Ik*k**8*((V(A2,A1)*V(A3,A2)*V(A4,A3)*V(A5,A4)*V(A6,A5)*V(A7,A6)*V(A8,A7)*V(A9,A8))**al)
+  }

* Supply
V_V1          0 A1 1000V
I_I1          0 A1 DC {Ik}

.END
```

Copyright © 2021 IEEE. Personal use is permitted. For any other purposes, permission must be obtained from the IEEE by emailing pubs-permissions@ieee.org.

This is the author's version of an article that has been published in this journal. Changes were made to this version by the publisher prior to publication.
The final version of record is available at http://dx.doi.org/10.1109/JSEN.2021.3062428

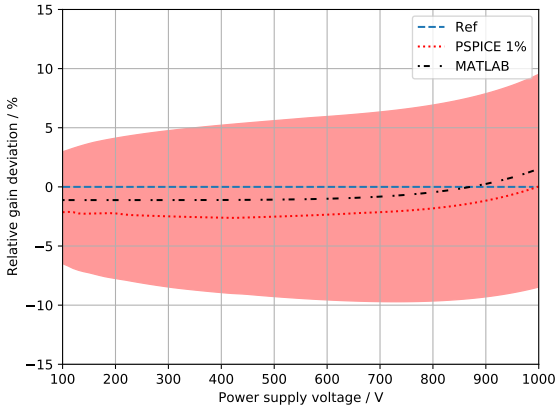

Fig. S2: PMT gain deviation $G/G_{\mathrm{Ref}} - 1$ of a passive divider network [1, Fig. 2b] as a function of total voltage bias V_{B} for a fixed (dark) photocathode current $I_{\mathrm{c}} = 10\,\mathrm{pA}$. G_{Ref} refers to the manufacturer gain (25). The blue dashed line depicts the gain according to the manufacturer (no deviation). The red dotted curve is the median measured with the PSPICE simulation using Monte Carlo statistical analysis for 100 runs, and the shaded area covers the region between the first and third quartiles. The dynode parameters $\alpha_i, k_i, i \in [1, N]$, cf. Listing 4 and [1, Fig. 3], have a mean value $\hat{\alpha} = 0.881$ and $\hat{k} = 0.0936$ and a tolerance of 1 %. For comparison, the MATLAB curve with 0 % tolerance is presented as black dash-dotted line.

Monte Carlo statistical analysis

The dynode model proposed by [1, Fig. 3] with auxiliary current sources and resistors with a predefined tolerance enables the use of Monte Carlo statistical analysis within PSPICE or NGSPICE. For the sake of clarity, we had focused on the average results with constant parameters: neither the NGSPICE, PSPICE or MATLAB calculations included stochastic repetitions with random variations of the dynode parameters within the central part of the manuscript.

A dedicated statistical analysis is presented here, with the corresponding PSPICE and NGSPICE circuits on Listings 4 and 5. It should be noted that, in the case of the NGSPICE subcircuit, the equations have to be tweaked for the solver to converge. The reason might be that the jacobian is presumably evaluated at initial inter-dynode voltages of $V_i = 0$, where the derivatives of the source equations contain a singularity in the term $V_i^{\alpha-1}$. All occurrences of V_i are thus changed with $V_i + 10^{-300}$ in Listing 5. In the case of PSPICE, this workaround is not necessary, but the $GMIN$ has to be lowered down to 10^{-18} if the recursive Listing 4 is used, as explained in Fig. S1.

The Monte Carlo statistical analysis of the simulated PMT gain using PSPICE is presented in Figs. S2 and S3 for 100 runs.

Listing 4: PSPICE netlist file of a PMT using the recursive formulation and auxiliary sources for Monte Carlo sampling of dynode parameters.

```
** Analysis setup **
.PARAM         Ik=10pA al=0.881 k=0.0936
.DC LIN PARAM Ik 1p 400p 1p
.OPTIONS GMIN=0.001f

* Passive divider network
R_R1          A2 A1   330k
R_R2          A3 A2   330k
R_R3          A4 A3   330k
R_R4          A5 A4   330k
R_R5          A6 A5   330k
R_R6          A7 A6   330k
R_R7          A8 A7   330k
R_R8          A9 A8   330k
R_R9          0 A9   160k

* Measure stage currents
V_V10          Cat A1 DC 0
V_V11          Dy1 A2 DC 0
V_V12          Dy2 A3 DC 0
V_V13          Dy3 A4 DC 0
V_V14          Dy4 A5 DC 0
V_V15          Dy5 A6 DC 0
V_V16          Dy6 A7 DC 0
V_V17          Dy7 A8 DC 0
V_V18          Dy8 A9 DC 0

* Amplification functions
G_G1          0 Dy1 VALUE { I(V_V10)*(V(k1)*V(A2,A1)**V(al1)-1) }
G_G2          0 Dy2 VALUE {
```

Copyright © 2021 IEEE. Personal use is permitted. For any other purposes, permission must be obtained from the IEEE by emailing pubs-permissions@ieee.org.

This is the author's version of an article that has been published in this journal. Changes were made to this version by the publisher prior to publication.
The final version of record is available at http://dx.doi.org/10.1109/JSEN.2021.3062428

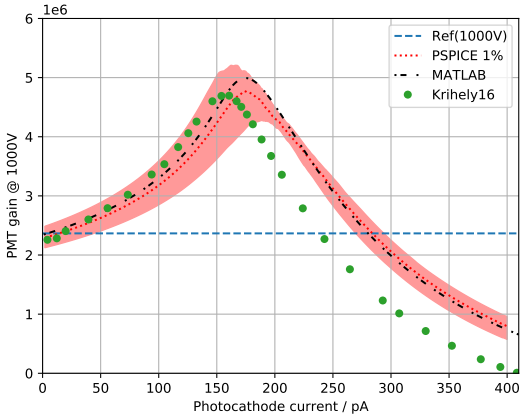

Fig. S3: PMT gain G of a passive divider network [1, Fig. 2b] as a function of photocathode current I_c for a fixed power supply voltage $V_B = 1000\,\mathrm{V}$. The blue dashed line depicts the gain according to the manufacturer. The red dotted curve is the median measured with the PSPICE simulation using Monte Carlo statistical analysis for 100 runs, and the shaded area covers the region between the first and third quartiles. The dynode parameters $\alpha_i, k_i, i \in [1, N]$, cf. Listing 4 and [1, Fig. 3], have a mean value $\hat{\alpha} = 0.881$ and $\hat{k} = 0.0936$ and a tolerance of 1 %. For comparison, the MATLAB curve with 0 % tolerance is presented as black dash-dotted line. The green circles are data points derived graphically from [2, Fig. 5a], that used $\alpha = 0.7843720$ and $k = 0.1213166$.

```
+  I(V_V11)/(1-1/(V(k1)*V(A2,A1)**V(al1)))*(V(k2)*V(A3,A2)**V(al2)-1) }
G_G3          0 Dy3 VALUE {
+  I(V_V12)/(1-1/(V(k2)*V(A3,A2)**V(al2)))*(V(k3)*V(A4,A3)**V(al3)-1) }
G_G4          0 Dy4 VALUE {
+  I(V_V13)/(1-1/(V(k3)*V(A4,A3)**V(al3)))*(V(k4)*V(A5,A4)**V(al4)-1) }
G_G5          0 Dy5 VALUE {
+  I(V_V14)/(1-1/(V(k4)*V(A5,A4)**V(al4)))*(V(k5)*V(A6,A5)**V(al5)-1) }
G_G6          0 Dy6 VALUE {
+  I(V_V15)/(1-1/(V(k5)*V(A6,A5)**V(al5)))*(V(k6)*V(A7,A6)**V(al6)-1) }
G_G7          0 Dy7 VALUE {
+  I(V_V16)/(1-1/(V(k6)*V(A7,A6)**V(al6)))*(V(k7)*V(A8,A7)**V(al7)-1) }
G_G8          0 Dy8 VALUE {
+  I(V_V17)/(1-1/(V(k7)*V(A8,A7)**V(al7)))*(V(k8)*V(A9,A8)**V(al8)-1) }
G_G9          0 0 VALUE { -I(V_V18)/(1-1/(V(k8)*V(A9,A8)**V(al8))) }

* Auxiliary DC sources for k and alpha sampling
I_I11         0 k1 DC 1
I_I12         0 k2 DC 1
I_I13         0 k3 DC 1
I_I14         0 k4 DC 1
I_I15         0 k5 DC 1
I_I16         0 k6 DC 1
I_I17         0 k7 DC 1
I_I18         0 k8 DC 1
I_I21         0 al1 DC 1
I_I22         0 al2 DC 1
I_I23         0 al3 DC 1
I_I24         0 al4 DC 1
I_I25         0 al5 DC 1
I_I26         0 al6 DC 1
I_I27         0 al7 DC 1
I_I28         0 al8 DC 1

* Resistors: modify them to apply desired tolerance
R_R11         k1 0 {k}
R_R12         k2 0 {k}
R_R13         k3 0 {k}
R_R14         k4 0 {k}
R_R15         k5 0 {k}
R_R16         k6 0 {k}
R_R17         k7 0 {k}
R_R18         k8 0 {k}
R_R21         al1 0 {al}
R_R22         al2 0 {al}
R_R23         al3 0 {al}
R_R28         al8 0 {al}
R_R27         al7 0 {al}
R_R26         al6 0 {al}
R_R25         al5 0 {al}
R_R24         al4 0 {al}
```

Copyright © 2021 IEEE. Personal use is permitted. For any other purposes, permission must be obtained from the IEEE by emailing pubs-permissions@ieee.org.

This is the author's version of an article that has been published in this journal. Changes were made to this version by the publisher prior to publication.
The final version of record is available at http://dx.doi.org/10.1109/JSEN.2021.3062428


```
* Supply
V_V1         0 A1 1000V
I_I1         0 Cat DC {Ik}

.END
```

Listing 5: NGSPICE subcircuit of a PMT using the recursive formulation and auxiliary sources for Monte Carlo sampling of dynode parameters.

```
*  NODE NUMBERS
*                           Dynode 1
*                           |   Dynode 2
*                           |   |   Dynode 3
*                           |   |   |   Dynode 4
*                           |   |   |   |   Dynode 5
*                           |   |   |   |   |   Dynode 6
*                           |   |   |   |   |   |   Dynode 7
*                           |   |   |   |   |   |   |   Dynode 8
*                           |   |   |   |   |   |   |   |   Cathode
*                           |   |   |   |   |   |   |   |   |   Anode
*                           |   |   |   |   |   |   |   |   |   |   Cathode current plus
*                           |   |   |   |   |   |   |   |   |   |   |    Cathode current minus
*                           |   |   |   |   |   |   |   |   |   |   |    |
.SUBCKT KRIHELY14_Dyn08_MC Dy1 Dy2 Dy3 Dy4 Dy5 Dy6 Dy7 Dy8 Cat Ano Scp  Scm    PARAMS: alpha=0.78 k=0.12
* alpha: dynode-specific parameter
* k: dynode-specific parameter

* Amplification functions
.func gvald(ip,alpha ,k         ,v,vp    )={ip*(k*(v-vp+1e-300)**alpha-1)                                    }
.func gval (ip,alphap,kp,alpha,k,v,vp,vpp)={ip*(k*(v-vp+1e-300)**alpha-1)/(1-1/(kp*(vp-vpp+1e-300)**alphap))}
.func gvala(ip,alphap,kp,alpha,k,v,vp,vpp)={ip                           /(1-1/(k *(vp-vpp+1e-300)**alpha ))}
*1e-300 needed to avoid singularity in derivative at zero

* Measure photocathode current
VMES0 Scm Cat 0
R0 Scp GND 0

* Measure stage currents
VMES1  SDy1 Dy1 0
VMES2  SDy2 Dy2 0
VMES3  SDy3 Dy3 0
VMES4  SDy4 Dy4 0
VMES5  SDy5 Dy5 0
VMES6  SDy6 Dy6 0
VMES7  SDy7 Dy7 0
VMES8  SDy8 Dy8 0
VMES20 SAno Ano 0

* Dynode amplification stages
G1  GND SDy1 GND GND value= gvald( I(VMES0), V(a1), V(k1),        V(Cat)                          )
G2  GND SDy2 GND GND value= gval(  I(VMES1), V(a1), V(k1), V(a2), V(k2), V(Dy2), V(Dy1), V(Cat) )
G3  GND SDy3 GND GND value= gval(  I(VMES2), V(a2), V(k2), V(a3), V(k3), V(Dy3), V(Dy2), V(Dy1) )
G4  GND SDy4 GND GND value= gval(  I(VMES3), V(a3), V(k3), V(a4), V(k4), V(Dy4), V(Dy3), V(Dy2) )
G5  GND SDy5 GND GND value= gval(  I(VMES4), V(a4), V(k4), V(a5), V(k5), V(Dy5), V(Dy4), V(Dy3) )
G6  GND SDy6 GND GND value= gval(  I(VMES5), V(a5), V(k5), V(a6), V(k6), V(Dy6), V(Dy5), V(Dy4) )
G7  GND SDy7 GND GND value= gval(  I(VMES6), V(a6), V(k6), V(a7), V(k7), V(Dy7), V(Dy6), V(Dy5) )
G8  GND SDy8 GND GND value= gval(  I(VMES7), V(a7), V(k7), V(a8), V(k8), V(Dy8), V(Dy7), V(Dy6) )
G20 SAno GND GND GND value= gvala( I(VMES8), V(a8), V(k8), V(a8), V(k8), V(Ano), V(Dy8), V(Dy7) )

* Auxiliary DC sources for k and alpha sampling
I1  GND k1 1
I2  GND k2 1
I3  GND k3 1
I4  GND k4 1
I5  GND k5 1
I6  GND k6 1
I7  GND k7 1
I8  GND k8 1
I11 GND a1 1
I12 GND a2 1
I13 GND a3 1
I14 GND a4 1
I15 GND a5 1
I16 GND a6 1
I17 GND a7 1
I18 GND a8 1

* Resistors: modify them to apply desired tolerance
R1  GND k1 {k}
R2  GND k2 {k}
R3  GND k3 {k}
R4  GND k4 {k}
R5  GND k5 {k}
R6  GND k6 {k}
R7  GND k7 {k}
```

Copyright © 2021 IEEE. Personal use is permitted. For any other purposes, permission must be obtained from the IEEE by emailing pubs-permissions@ieee.org.

This is the author's version of an article that has been published in this journal. Changes were made to this version by the publisher prior to publication.
The final version of record is available at http://dx.doi.org/10.1109/JSEN.2021.3062428


```
R8  GND k8 {k}
R11 GND a1 {alpha}
R12 GND a2 {alpha}
R13 GND a3 {alpha}
R14 GND a4 {alpha}
R15 GND a5 {alpha}
R16 GND a6 {alpha}
R17 GND a7 {alpha}
R18 GND a8 {alpha}

.ENDS
```

Copyright © 2021 IEEE. Personal use is permitted. For any other purposes, permission must be obtained from the IEEE by emailing pubs-permissions@ieee.org.